Science of the Total Environment 500–501 (2014) 361–372

Contents lists available at ScienceDirect

Science of the Total Environment

journal homepage: www.elsevier.com/locate/scitotenv

Fingerprinting sedimentary and soil units by their natural metal contents: A new approach to assess metal contamination

Alessandro Amorosi [a,*], Marina Guermandi [b], Nazaria Marchi [b], Irene Sammartino [c]

[a] Department of Biology, Earth and Environmental Sciences, University of Bologna, Via Zamboni 67, 40127 Bologna, Italy
[b] Geological, Seismic and Soil Survey, Regione Emilia-Romagna, Viale della Fiera 8, 40127 Bologna, Italy
[c] Geologic Consultant, Via Brizio 17/3, 40134 Bologna, Italy

HIGHLIGHTS

- Sedimentary facies and soil units are fingerprinted by their natural metal contents.
- Source-rock composition, grain size and soil weathering control metal distribution.
- Background concentrations of Cr and Ni commonly exceed the Italian guidelines.
- Predetermined background values are inadequate to depict local pollution.
- Geochemical maps based on soil/geological data allow assessing metal contamination.

ARTICLE INFO

Article history:
Received 2 June 2014
Received in revised form 31 July 2014
Accepted 23 August 2014
Available online xxxx

Editor: F.M. Tack

Keywords:
Natural background
Alluvial plain
Metal pollution
Soil contamination
Geochemical map
Po Plain

ABSTRACT

One of the major issues when assessing soil contamination by inorganic substances is reliable determination of natural metal concentrations. Through integrated sedimentological, pedological and geochemical analyses of 1414 (topsoil/subsoil) samples from 707 sampling stations in the southern Po Plain (Italy), we document that the natural distribution of five potentially toxic metals (Cr, Ni, Cu, Zn and Pb) can be spatially predicted as a function of three major factors: source-rock composition, grain size variability and degree of soil weathering. Thirteen genetic and functional soil units (GFUs), each reflecting a unique combination of these three variables, are fingerprinted by distinctive geochemical signatures. Where sediment is supplied by ultramafic (ophiolite-rich) sources, the natural contents of Cr and Ni in soils almost invariably exceed the Italian threshold limits designated for contaminated lands (150 mg/kg and 120 mg/kg, respectively), with median values around twice the maximum permissible levels (345 mg/kg for Cr and 207 mg/kg for Ni in GFU B5). The original provenance signal is commonly confounded by soil texture, with general tendency toward higher metal concentrations in the finest-grained fractions. Once reliable natural metal concentrations in soils are established, the anthropogenic contribution can be promptly assessed by calculating metal enrichments in topsoil samples. The use of combined sedimentological and pedological criteria to fingerprint GFU geochemical composition is presented here as a new approach to enhance predictability of natural metal contents, with obvious positive feedbacks for legislative purposes and environmental protection. Particularly, natural metal concentrations inferred directly from a new type of pedogeochemical map, built according to the international guideline ISO 19258, are proposed as an efficient alternative to the pre-determined threshold values for soil contamination commonly established by the national regulations.

© 2014 Elsevier B.V. All rights reserved.

1. Introduction

The assessment of soil contamination by risk elements and the estimate of anthropogenic disturbance are increasingly important issues when dealing with environmental problems. In this regard, establishing the natural concentrations of potentially toxic metals with respect to the anthropogenic contribution is essential for defining the pollution status of soils, and thus developing adequate policies of environmental protection (Salminen and Tarvainen, 1997). Total element concentrations in the natural environments may vary by several orders of magnitude (Blaser et al., 2000; Tarvainen and Kallio, 2002). This is especially true for certain metals, such as Cr and Ni, whose naturally elevated concentrations in ultramafic rocks can be orders of magnitude higher than values

* Corresponding author. Tel.: +39 051 2094586; fax: +39 051 2094522.
E-mail addresses: alessandro.amorosi@unibo.it (A. Amorosi), MGuermandi@regione.emilia-romagna.it (M. Guermandi), NMarchi@regione.emilia-romagna.it (N. Marchi), irene.sammartino@gmail.com (I. Sammartino).

http://dx.doi.org/10.1016/j.scitotenv.2014.08.078
0048-9697/© 2014 Elsevier B.V. All rights reserved.

from continental crust rocks (Hiscott, 1984). As a consequence, natural metal concentrations in soils may vary markedly from area to area, within a region and between regions, making definition of global background values impossible (Reimann and Garrett, 2005).

The Po Plain, one of the widest alluvial plains in Europe, is a heavily urbanized area that hosts about one third of the Italian population. This region is characterized by intense agricultural and industrial activities, and for this reason it is seriously at risk of metal pollution. Recent studies carried out south of Po River (Emilia-Romagna plain), have documented that Cr and Ni, among all potentially toxic metals, may serve as powerful tracers of sediment provenance, and that they play a major role for the reconstruction of sediment dispersal patterns throughout the system (Amorosi et al., 2002, 2008; Curzi et al., 2006; Amorosi, 2012; Bianchini et al., 2013, 2014). Particularly, relatively high Cr and Ni values in alluvial and coastal plain sediment have been inferred to reflect the abundance of ultramafic detritus supplied by the Po River via its tributaries that drain the ophiolitic complexes of the Western Alps and NW Apennines (Fig. 1). Such "anomalous" high concentrations may exceed the national standards for potentially toxic metals (Bianchini et al., 2002; Amorosi and Sammartino, 2007), and for this reason they are a matter of concern and a serious problem for the environmental agencies.

A huge amount of data produced in the Emilia-Romagna plain in the framework of soil (Regione Emilia-Romagna, 2010) and geological (Regione Emilia-Romagna, 1999) mapping projects allows today to examine the natural distribution of selected elements within a mixed pedological and geological framework, through integration of geochemical data with detailed soil and facies characterization.

A general framework for standardizing methods for geochemical mapping at the global–regional scale has been developed during the 1990s (Darnley, 1997; Plant et al., 1997; Salminen and Tarvainen, 1997). However, there is still no established technique for mapping geochemical data, and an integrated system of geochemical mapping with detailed geological and soil data is far from being achieved. The vast majority of the existing geochemical maps is built on either single point representations or computer-assisted, geostatistical interpolation methods (see Reimann and Filzmoser, 2000; Reimann et al., 2002; Cheng, 2007; Micó et al., 2008, for a review of the statistical approaches). A pure statistical approach, however, in general fails to consider soil and geological properties and, as such, cannot provide adequate representation of spatial metal distribution away from the sites where data are available. In these types of geochemical maps, delineation of class boundaries may represent a highly subjective and interpretive exercise, and the resulting maps can hardly meet the needs of land-use planning.

The major objectives of this work, which focuses on a wide spectrum of alluvial, deltaic and coastal deposits, are: (i) to assess the controlling factors of natural metal distribution in the southern Po Plain, (ii) to document the possibility of fingerprinting sedimentary and soil units by their natural metal contents, and (iii) to show to what extent a new type of pedogeochemical map (Regione Emilia-Romagna, 2012), largely based on sedimentological and soil properties, may impact the determination of natural metal concentrations and the reliable estimates of anthropogenic pollution.

We use here the term "pedogeochemical content" (or "natural background value", according to the international guideline ISO, 19258, 2005) to refer to metal contents resulting from natural geological and pedological processes, excluding any addition of human origin (Micó et al., 2008). This term is commonly referred to by the geochemists as "background value" (Lepeltier, 1969; Rose et al., 1979; Reimann and Garrett, 2005), and varies according to the nature of the parent material for any particular element. The "pedogeochemical content" is conceptually separated from the term "baseline" (or "usual background value" of ISO, 19258, 2005), which is commonly meant to define a concentration of a substance that includes a diffuse anthropogenic contribution due to atmospheric deposition and agricultural practice (Tarvainen and Kallio, 2002; Cicchella et al., 2005; Albanese et al., 2007).

2. Geological setting

The Po Plain is the superficial expression of a subsiding foreland basin (Po River Basin) of Pliocene to Quaternary age. It is made up of the longest Italian river (the Po), 652 km long, which flows in W-E direction from the Western Alps to the Adriatic Sea, and by a series of transverse tributaries. The Po Plain is bounded by two mountain chains: the Alps to the north, and the Apennines to the south (Fig. 1). The Alpine catchments show contrasting compositional signatures, which reveal the complex geological history of this orogen. Two major structural

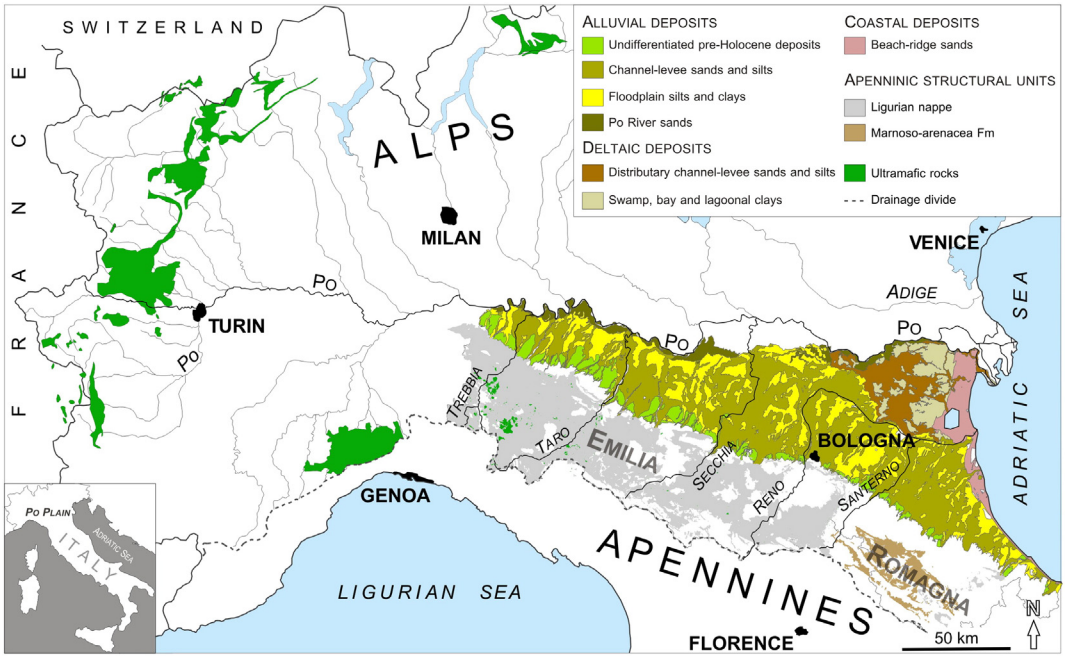

Fig. 1. Simplified geological map of the Emilia-Romagna plain (modified from Regione Emilia-Romagna, 1999) and adjoining areas.

units are recognized in the Apenninic catchments: the Ligurian nappe (Fig. 1), cropping out approximately between Trebbia and Santerno Rivers (Emilia Apennines), includes different fault-bounded structural units and is made up of ophiolites and weakly- or non-metamorphosed sedimentary rocks of Cretaceous to Miocene age (Pini, 1999). Between the Santerno River and the Adriatic Sea (Romagna Apennines in Fig. 1), the Apenninic river catchments are made up, instead, of a homogeneous turbiditic unit of Miocene age ("Marnoso-arenacea Formation" – Ricci Lucchi, 1986).

The Emilia-Romagna plain, south of Po River, has a surface area of 11,600 km^2. From a sedimentological perspective, it includes three depositional systems, corresponding to alluvial, deltaic, and coastal plain deposits, respectively (Fig. 1). These depositional systems, in turn, include a variety of facies associations, formed in distinct depositional environments.

Undifferentiated alluvial deposits of pre-Holocene age crop out at the basin margin, where the Apenninic rivers enter the alluvial plain (Ori, 1993; Picotti and Pazzaglia, 2008; Amorosi et al., 2014; Gunderson et al., 2014). The bulk of the plain consists of alluvial deposits supplied by about 25 river systems. These deposits are subdivided into coarser, near-channel (crevasse and levee) sands and silts, with lateral transition to overbank fines (silts and clays). Thick, amalgamated sand bodies attributable to the Po River are present at the northern margin of the study area, where they form a W-E trending channel belt that roughly coincides with the axis of the present Po River course. The alluvial deposits show downstream transition to deltaic and coastal facies associations (Fig. 1). An abandoned Po Delta lobe, which was active up to the XII century A.D. (Bondesan et al., 1995; Correggiari et al., 2005), is clearly identifiable S-W of the modern delta (Fig. 1). Deltaic deposits include distributary-channel sands and interdistributary (swamp, bay and lagoonal) clays. Coastal deposits consist almost entirely of sand beach-ridge deposits (nearshore to aeolian facies associations) of post-Roman age, elongated parallel to the present shoreline (Fig. 1). These beach-ridges which, at least in part, correspond to delta front deposits, show contrasting (Po River versus Apenninic) source-rock compositions (Marchesini et al., 2000; Amorosi et al., 2007). Changes in sediment provenance reflect the abandonment of previously active Po Delta distributary channels and their subsequent incorporation into the Apenninic fluvial network (Veggiani, 1974).

3. Genetic and functional soil units

The Soil Map of the Emilia-Romagna plain at 1:50,000 scale (Regione Emilia-Romagna, 2012) consists of 295 soil typological units. Based upon integrated pedological and geological criteria, these units were grouped into a set of thirteen homogeneous, higher-rank soil units, namely Genetic and functional soil units (GFUs in Fig. 2). The following distinctive characteristics were used to assemble individual GFUs (Table 1): soil texture, degree of soil weathering, sediment provenance and depositional environment (facies association). Each GFU is fingerprinted by a unique combination of the above features (Table 1).

On the basis of grain size variability, four types of GFUs were differentiated: (i) fine-grained soil units (GFUs "A" in Table 1), including a mixture of clay and silt in different proportions; (ii) moderately fine to moderately coarse-grained soil units (GFUs "B" in Table 1), made up predominantly of sandy silt and silty sand, with subordinate very fine and fine sand; (iii) coarse-grained soil units (GFUs "C" in Table 1), consisting of fine to very coarse sand; (iv) GFU D1, characterized by an abundance of organic-rich clay. In general, the soils of the Emilia-Romagna plain have poorly weathered profiles. Superficial deposits date back primarily to the post-Roman period, which accounts for their commonly low to moderate degree of weathering (Table 1). A very low degree of weathering is recorded uniquely in GFUs C1, C2 and D1, where soils developed on surfaces exposed for a few centuries only. In contrast, soils with relatively high degree of weathering (e.g. Luvisols of WRB IUSS Working Group, 2006) crop out exclusively at the basin margin (UGF A1 in Table 1), where deposits are commonly of pre-Holocene age.

GFUs were further differentiated on the basis of their parent material, i.e., sediment provenance (Table 1). Of particular interest for the geochemical characterization of the Emilia-Romagna plain is the presence in selected river catchments of ultramafic (ophiolitic) complexes that supply Cr-rich and Ni-rich detritus to the alluvial and coastal system (Amorosi and Sammartino, 2007). Ophiolitic rocks crop out extensively in the Western Alps and in the NW portion of the Apennines, between Trebbia and Taro rivers (Fig. 1). As a consequence, abundant ophiolitic detritus is recorded in alluvial (GFU B4 in Table 1), deltaic (A4, B6, D1) and coastal (C2) deposits fed by Po river, and in the NW part of the Emilia-Romagna plain (A4, B5).

Finally, soil units were also classified based on their sedimentological characteristics (Table 1) into three depositional systems (fluvial, deltaic and coastal – see previous section) which, in turn, were subdivided into six facies associations (fluvial channel, floodplain, distributary channel, interdistributary area, interdistributary bay, and beach ridge deposits – Fig. 1).

4. Materials and methods

For this study, we followed ISO 19258 (2005) standards, from sample collection to the statistical treatment of data. Soil and lithofacies assignments were based on field descriptions, implemented by a large amount of pedological, geomorphological and sedimentological data,

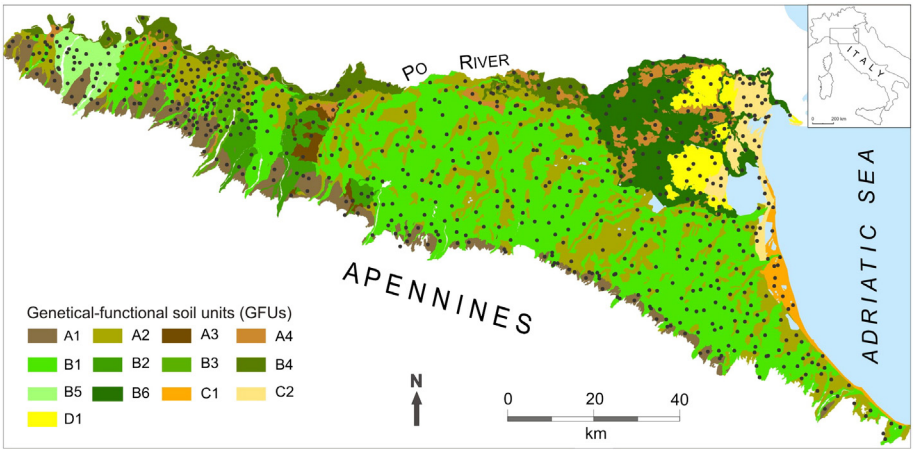

Fig. 2. Genetic and functional soil units (GFUs) and their spatial distribution in the Emilia-Romagna plain (based upon Regione Emilia-Romagna, 1999, 2010). For GFUs description, see Table 1. Black dots indicate sampling sites. (For interpretation of the references to color in this figure legend, the reader is referred to the web version of this article.)

Table 1
GFU classification as a function of soil type (IUSS Working Group WRB, 2006), sediment provenance (Po River catchment encompasses both Alpine and Apenninic river catchments) and depositional environment/facies association.

	GFU	Soil type	Sediment provenance	Facies association
A	A1	Medium-to fine textured, high degree of soil weathering Stagnic Luvisols, Vertic Cambisols	Apenninic catchment. Variable ophiolitic supply	Undifferentiated alluvial
	A2	Fine textured, low to moderate degree of soil weathering Vertic Cambisols, Hyposalic Vertisols, Calcic Vertisols	Apenninic catchment. No ophiolitic supply	Floodplain
	A3	Fine textured, low to moderate degree of soil weathering Vertic Cambisols, Calcic Vertisols, Eutric Vertisols	Mixed Po/apenninic. Moderate to high ophiolitic supply	Floodplain
	A4	Fine textured, low to moderate degree of soil weathering Vertic Cambisols, Calcic Vertisols, Hyposalic Vertisols	Po River catchment	Interdistributary area (upper delta plain)
B	B1	Moderately fine-textured to moderately coarse-textured, with rare gravels, low to moderate degree of soil weathering Haplic Cambisols, Haplic Calcisols	Apenninic catchment. No ophiolitic supply	Channel-levee, crevasse
	B2	Moderately fine-textured to moderately coarse-textured, with rare gravels, low to moderate degree of soil weathering Haplic Cambisols, Haplic Calcisols	Apenninic catchment. Moderate ophiolitic supply	Channel-levee, crevasse
	B3	Moderately fine-textured to moderately coarse-textured, with rare gravels, low to moderate degree of soil weathering Haplic Cambisols, Haplic Calcisols	Apenninic catchment. Moderate to high ophiolitic supply	Channel-levee, crevasse
	B4	Medium- to moderately coarse textured, low to moderate degree of soil weathering Haplic Cambisols, Haplic Calcisols	Po River catchment	Channel-levee, crevasse
	B5	Moderately fine-textured to moderately coarse-textured, with abundant gravels, low to moderate degree of soil weathering Haplic Cambisols, Haplic Calcisols	Apenninic catchment. High ophiolitic supply	Channel-levee, crevasse
	B6	Medium- to moderately coarse textured, low to moderate degree of soil weathering Haplic Cambisols, Haplic Calcisols	Po River catchment	Distributary channel-levee, crevasse
C	C1	Coarse textured, low degree of soil weathering Endogleyic Arenosols	Apenninic catchment. No ophiolitic supply	Beach ridge (coastal plain)
	C2	Coarse textured, low degree of soil weathering Endogleyic Arenosols	Po River catchment	Beach ridge (delta front)
D	D1	Organic material, Thionic Histosols, Thionic Fluvisols	Po River catchment	Interdistributary bay (lower delta plain)

summarized by the Soil Map at 1:50,000 scale (Regione Emilia-Romagna, 2010) and the Geological Map of the Po Plain at 1:250,000 scale (Regione Emilia-Romagna, 1999), respectively. In addition, we used the Geological Map of the Emilia-Romagna region at 1:10,000 scale in its Apenninic foothills portion, along with the Map of the Drainage Basins, the Soil Use Map (1976–2008) and several sets of aerial photographs (1954–2008), which were used to establish precise relationships between sampling sites and modern/past soil use.

4.1. Sampling

A homogeneous geochemical dataset was obtained from 707 sampling stations, with overall density of about 1 sample per 16 km^2. Sampling did not follow regular grids, but was set up to provide a geographic coverage of sedimentary and soil units defined by the thirteen GFUs (Fig. 2). The number of samples for individual GFU varies between 17 (B2 in Table 2) and 198 (B1 in Table 2).

Two soil samples were collected at each study site by hand drilling, at depths of 20–30 cm and 90–140 cm, respectively, using Eijkelkamp Agrisearch equipment (01.11.SO hand auger set for heterogeneous soils). Samples from the deeper soil horizon (e.g., the C horizon) were used for the determination of the pedogeochemical content (Blaser et al., 2000), whereas samples collected in the depth of 20–30 cm were used for the detection of geochemical anomalies. ISO 19258 (2005) indicates depths below 40 cm in agricultural soils and for inorganic compounds to be representative of natural contents. Since agricultural practices (vineyards) in the study area may have impact on soil down to 80 cm in depth, we assumed that samples collected below 80 cm depth had no significant anthropogenic influence (Huisman et al., 1997; ISO, 19258, 2005). In addition, we performed detailed comparison with existing geochemical data from 30 to 150 m deep boreholes from the same area (Amorosi et al., 2002, 2007), which helped establish a representative natural background dataset.

At each sampling site the following general information was annotated: location, elevation, soil slope, soil use, stratigraphic unit. Core descriptions also included: grain size, color, reaction to hydrochloric acid, pH (in soils with high organic content), accessory components (plant fragments, wood, fossils, carbonate nodules, etc). All field data were stored in a GIS database.

4.2. Geochemical analyses

To determine total metal concentrations, following ISO 19258 (2005) 1414 samples were analyzed by X-ray fluorescence (XRF). XRF analyses were conducted at Bologna University laboratories. Samples, pressed into tablets, were analyzed for 10 major and 16 trace elements in a Philips PW1480 spectrometry with a Rh tube, using matrix correction methods of Franzini et al. (1972) and Leoni et al. (1982). Reference samples, including samples BR, BCR-1, W1, TB, NIM-P, DR-N, KH and AGV-1 (Govindarajiu, 1989) were also analyzed. The estimated precision and accuracy for trace element determinations, based on the reference standards, are better than 5%, except for those elements at 10 ppm and lower

(10–15%). Loss on ignition (LOI) was evaluated after overnight heating at 950 °C.

In order to compare XRF data with another technique of metal determination commonly used for geochemical mapping purposes, the whole set of topsoil analyses (707 samples) was replicated by aqua regia inductively coupled plasma mass spectrometry (ICP-MS). Several studies have documented that concentrations of certain trace metals (such as Cr and Ni) determined using aqua regia extractions can be significantly lower than total concentrations based upon XRF spectrometry. In particular, lower Cr extractability using aqua regia has been shown by Tarvainen et al. (2009), and similar results have also been reported by Sterckemann et al. (1996) and Amorosi and Sammartino (2011), who demonstrated remarkably lower levels (30–60% relative to XRF) of aqua regia extractions for Cr and Ni.

Aqua regia extractions were performed mostly (607 samples) at the Regional Environmental Agency (ARPA) laboratories in Ravenna (Italy), following UNIEN 13346 standard method, whereas 100 ICP-MS analyses were carried out at Als Chemex laboratories in Vancouver (Canada), following ME-MS41 procedure (for the latter, see Amorosi and Sammartino, 2011).

Detailed comparison between XRF and aqua regia extraction techniques is beyond the scope of our paper, and for this reason the results of ICP-MS analyses are not shown here. However, we report the following mean percentages (relative to XRF determinations) of metals extracted from the 707 study samples following aqua regia digestion: Cr 69%, Ni 72%, Zn 82%, Cu 83%, and Pb 108%. Given the specific environmental interest for Cr and Ni, whose concentrations in Po Plain soils may commonly exceed the threshold values (see Section 1), determination of metals using aqua regia extractions appeared very arguable. For this reason, we selected XRF spectrometry as more suitable analytical technique for estimating natural background values of potentially toxic metals.

4.3. Statistical analysis

A combination of different graphics, including frequency histograms, cumulative frequency curves and box-plots was used to get the data distribution for each GFU (Reimann and Filzmoser, 2000; ISO, 19258, 2005; APAT, 2006; ARPAV, 2011). However, in order to test the hypothesis that cumulative distributions could be modeled as standard normal or log-normal distributions, we applied to the GFU datasets the more formal Kolmogorov–Smirnov (K–S) test. The null hypothesis of normal distribution, calculated for all 13 GFUs and 5 metals, was accepted by 59 out of 65 combinations, with P-values > 0.05. To the other six datasets, the Box–Cox transformation was tested to approach a normal distribution. The identification of potential outliers was then performed through box-and-whiskers plots, where values exceeded 1.5 times the interquartile range (difference between the 75th and 25th percentiles). On the six datasets subject to the Box–Cox transformation, two groups of outliers were calculated, on both transformed and unmodified data. The outliers were then identified and excluded from the calculation of the pedogeochemical contents.

Following outlier removal, descriptive statistics was carried out for each metal, leading to UGFs characterization in terms of: number of detects, minimum detected concentration, maximum detected concentration, sum, mean, standard error, variance, standard deviation, median, skewness, kurtosis and geometric mean (Table 2). In order to ascertain the pedogeochemical content of Cr, Ni, Zn, Cu and Pb in the 13 GFUs, we calculated the 90th percentile (following recommendations from ISO, 19258, 2005) and the 95th percentile (Ander et al., 2013). The latter was used to develop regional estimates of natural background values in the study area, as carried out by Italian environmental agencies (APAT, 2006; ARPAV, 2011) and outlined in Section 6.

Given the potential impact of background determinations on environmental legislative measures, we applied the mechanical removal of certain outliers from the dataset as precautionary approach (recommended by ISO, 19258, 2005). For the same prudential reason, though we are inclined to think that the whole population of a given GFU represents the background population, following the Italian guidelines we used the 95th percentiles as natural background values.

5. Factors controlling spatial metal distribution

The combined sedimentological, pedological and geochemical characterization of the 13 GFUs shows that natural metal concentrations are not randomly distributed, but vary spatially in a consistent manner as a function of several parameters. Three variables (source-rock composition, grain size and the degree of soil weathering) appear as the major controlling factors of spatial metal distribution in the study area. The following sections explore selected geochemical features through a selection of binary plots that summarize to what extent elemental data can be used to develop a chemical fingerprint for each GFU.

5.1. Source-rock composition

As documented from distinct sectors of the Po Plain (Amorosi et al., 2002; Bianchini et al., 2002; Amorosi and Sammartino, 2007), Cr and Ni may act as powerful source discriminants across the sediment routing system. However, since variability in sediment texture can have a severe impact on provenance reconstructions, in order to compensate for grain size variations we normalized geochemical data using one element as grain size proxy (Loring, 1991; Daskalakis and O'Connor, 1995). Aluminum is commonly used as an efficient normalization factor (Covelli and Fontolan, 1997; Menon et al., 1998; Liaghati et al., 2003), and the Cr/Al_2O_3 ratio has been tested successfully for the discrimination of ultramafic versus non-ultramafic source-rock composition in Po Plain sediments (Dinelli et al., 2007; Amorosi, 2012). In this study, however, we used the Cr/V ratio (Amorosi and Sammartino, 2007), which proved considerably more efficient than any other parameter.

Application of the Cr/V diagram to subsoil samples, 90–140 cm deep, reveals that GFUs with highly contrasting ultramafic signature are aligned along two distinct regression straight lines (Fig. 3, left). These lines display a marked shift in Cr concentrations, reflecting sediment composition from two separate source areas.

The high Cr concentrations recorded within the Po River and Po Delta sediments (GFUs C2, B4, B6 and A4 in Fig. 3, left) are inferred to reflect erosion of Cr-rich ultramafic rocks exposed in the Po River catchment (Fig. 1). In contrast, relatively lower Cr values (GFUs C1, B1 and A2 in Fig. 3, left) are invariably recorded where sediment is supplied by ophiolite-free, Apenninic sources (see beach-ridge, channel-levee and floodplain facies associations in Fig. 1). The significant Cr enrichment at the northwestern tip of the Apennines (see scattered samples from GFU B5 in Fig. 3, left) is likely to reflect close proximity of alluvial plain deposits to the Apenninic sources of ultramafic detritus (Trebbia River catchment in Fig. 1). Short fluvial transport is also suggested by the abundance of serpentinite rock fragments reported from core descriptions.

Nickel confirms its expected geochemical behavior, showing positive covariance with Cr and similar patterns of spatial distribution throughout the study area (Fig. 4). Ni is a common substitution in Cr-spinel, potentially accounting for its high concentrations in ophiolite-fed detritus, and may also be resident in chlorite, another indicator of ultramafic provenance (Ratcliffe et al., 2007).

5.2. Soil texture

Hydraulic processes are one of the most influential features in sediment composition, because they fractionate the relative abundance of minerals with different hydraulic behavior (Morton and Hallsworth, 1999). This implies that the distribution of selected elements (and metals) can be markedly grain size dependent (Garcia et al., 2004; Garzanti et al., 2009). Several studies have documented the general

Table 2
Calculated descriptive summary statistics for the 13 GFUs and the five metals considered in this study. N is the number of subsoil samples (90–140 cm deep) analyzed for each GFU. Minimum value (Min), maximum value (Max), sum, mean, standard error, variance, standard deviation, median and geometric mean (Geom. mean) are expressed as mg/kg.

Chromium	*A1*	*A2*	*A3*	*A4*	*B1*	B2	B3	B4	B5	B6	C1	C2	D1
N	*71*	*138*	*25*	*21*	*197*	*17*	*29*	*33*	*23*	*41*	*18*	*55*	*19*
Min	*113*	*99*	*152*	*173*	*66*	*130*	*145*	*159*	*196*	*156*	*50*	*96*	*130*
Max	*184*	*169*	*272*	*273*	*151*	*192*	*244*	*250*	*646*	*256*	*82*	*167*	*273*
Sum	*10,525*	*18,636*	*5118*	*4854*	*21,411*	*2637*	*5363*	*6841*	*8352*	*8179*	*1101*	*7242*	*3769*
Mean	*148.24*	*135.04*	*204.72*	*231.14*	*108.69*	*155.12*	*184.93*	*207.30*	*363.13*	*199.49*	*61.17*	*131.67*	*198.37*
Std. error	*1.80*	*1.28*	*6.91*	*5.54*	*1.29*	*4.20*	*5.45*	*3.77*	*26.97*	*3.40*	*2.22*	*2.16*	*7.84*
Variance	*231.10*	*225.95*	*1194.29*	*644.63*	*326.08*	*299.99*	*860.71*	*469.72*	*16,732.80*	*473.81*	*89.09*	*257.34*	*1168.13*
Stand. dev	*15.20*	*15.03*	*34.56*	*25.39*	*18.06*	*17.32*	*29.34*	*21.67*	*129.36*	*21.77*	*9.44*	*16.04*	*34.18*
Median	*148*	*137*	*197*	*237*	*108*	*153*	*180*	*209*	*345*	*203*	*60*	*132*	*199*
Skewness	*0.06*	*−0.44*	*0.49*	*−0.37*	*0.03*	*0.37*	*0.54*	*−0.11*	*0.40*	*0.16*	*0.70*	*0.02*	*0.19*
Kurtosis	*−0.03*	*−0.42*	*−0.94*	*−0.59*	*−0.23*	*−0.86*	*−1.07*	*−0.37*	*−0.86*	*−0.23*	*−0.52*	*−0.37*	*−0.13*
Geom. mean	*147.46*	*134.17*	*202.02*	*229.76*	*107.15*	*154.23*	*182.78*	*206.18*	*341.22*	*198.33*	*60.52*	*130.70*	*195.54*
Nickel													
N	*70*	*137*	*23*	*19*	*197*	*17*	*29*	*33*	*23*	*41*	*19*	*60*	*19*
Min	*37*	*59*	*108*	*131*	*37*	*82*	*101*	*111*	*145*	*95*	*22*	*52*	*100*
Max	*111*	*107*	*194*	*187*	*101*	*110*	*151*	*179*	*387*	*191*	*41*	*113*	*152*
Sum	*5266*	*11,424*	*3257*	*3064*	*13,489*	*1652*	*3622*	*4736*	*5196*	*5667*	*628*	*4506*	*2368*
Mean	*75.23*	*83.39*	*141.61*	*161.26*	*68.47*	*97.18*	*124.90*	*143.52*	*225.91*	*138.22*	*33.05*	*75.10*	*124.63*
Std. error	*1.88*	*0.81*	*4.64*	*3.62*	*0.87*	*2.13*	*2.53*	*2.89*	*13.89*	*3.53*	*1.23*	*1.93*	*3.18*
Variance	*248.64*	*90.27*	*495.89*	*249.21*	*150.16*	*77.40*	*185.45*	*275.82*	*4439.81*	*509.58*	*28.83*	*224.16*	*192.14*
Stand. dev	*15.77*	*9.50*	*22.27*	*15.79*	*12.25*	*8.80*	*13.62*	*16.61*	*66.63*	*22.57*	*5.37*	*14.97*	*13.86*
Median	*75*	*83*	*134*	*164*	*68*	*95*	*121*	*144*	*207*	*142*	*34*	*75*	*125*
Skewness	*0.05*	*0.20*	*0.57*	*−0.31*	*0.08*	*0.09*	*0.22*	*−0.04*	*0.89*	*0.00*	*−0.36*	*0.54*	*0.19*
Kurtosis	*0.03*	*−0.15*	*−0.56*	*−0.73*	*0.19*	*−1.50*	*−1.11*	*−0.64*	*−0.20*	*−0.77*	*−0.96*	*−0.02*	*−0.66*
Geom. mean	*73.51*	*82.85*	*140.00*	*160.51*	*67.34*	*96.80*	*124.19*	*142.57*	*217.53*	*136.38*	*32.61*	*73.68*	*123.90*
Zinc													
N	*75*	*132*	*23*	*19*	*198*	*18*	*29*	*34*	*23*	*41*	*19*	*58*	*20*
Min	*52*	*75*	*64*	*112*	*43*	*52*	*60*	*39*	*74*	*63*	*30*	*34*	*62*
Max	*111*	*126*	*128*	*167*	*111*	*106*	*108*	*124*	*108*	*166*	*46*	*59*	*156*
Sum	*6018*	*13,040*	*2241*	*2652*	*15,281*	*1489*	*2395*	*2946*	*2094*	*4213*	*711*	*2610*	*2298*
Mean	*80.24*	*98.79*	*97.43*	*139.58*	*77.18*	*82.72*	*82.59*	*86.65*	*91.04*	*102.76*	*37.42*	*45.00*	*114.90*
Std. error	*1.40*	*0.92*	*3.48*	*3.46*	*0.95*	*3.44*	*2.29*	*3.55*	*2.05*	*3.57*	*1.08*	*0.80*	*5.44*
Variance	*146.78*	*111.10*	*279.08*	*228.04*	*179.12*	*212.92*	*152.47*	*427.87*	*96.41*	*523.34*	*22.15*	*36.70*	*592.41*
Stand. dev	*12.12*	*10.54*	*16.71*	*15.10*	*13.38*	*14.59*	*12.35*	*20.69*	*9.82*	*22.88*	*4.71*	*6.06*	*24.34*
Median	*79*	*99*	*98*	*138*	*77*	*82*	*82*	*82.5*	*92*	*104*	*38*	*44.5*	*121.5*
Skewness	*0.19*	*−0.09*	*−0.13*	*0.06*	*−0.24*	*−0.16*	*0.19*	*−0.13*	*0.07*	*0.27*	*0.02*	*0.30*	*−0.66*
Kurtosis	*−0.28*	*−0.30*	*−0.63*	*−0.66*	*−0.15*	*−0.88*	*−0.86*	*−0.60*	*−1.24*	*0.00*	*−1.08*	*−0.42*	*−0.18*
Geom. mean	*79.33*	*98.22*	*96.00*	*138.80*	*75.94*	*81.44*	*81.70*	*84.02*	*90.54*	*100.23*	*37.14*	*44.60*	*112.02*
Copper													
N	*71*	*135*	*23*	*21*	*191*	*18*	*27*	*36*	*22*	*35*	*18*	*51*	*18*
Min	*13*	*24*	*26*	*32*	*14*	*28*	*26*	*9*	*27*	*26*	*9*	*3*	*20*
Max	*42*	*55*	*54*	*61*	*52*	*52*	*56*	*52*	*44*	*51*	*25*	*15*	*58*
Sum	*1822*	*5239*	*915*	*991*	*6384*	*673*	*1051*	*1178*	*816*	*1322*	*281*	*442*	*648*
Mean	*25.66*	*38.81*	*39.78*	*47.19*	*33.42*	*37.39*	*38.93*	*32.72*	*37.09*	*37.77*	*15.61*	*8.67*	*36.00*
Std. error	*0.80*	*0.49*	*1.67*	*1.44*	*0.55*	*1.68*	*1.35*	*1.68*	*1.05*	*1.06*	*0.99*	*0.41*	*2.10*
Variance	*45.91*	*32.20*	*63.91*	*43.26*	*57.72*	*50.60*	*49.38*	*101.24*	*24.47*	*39.59*	*17.55*	*8.51*	*79.41*
Stand. dev	*6.78*	*5.67*	*7.99*	*6.58*	*7.60*	*7.11*	*7.03*	*10.06*	*4.95*	*6.29*	*4.19*	*2.92*	*8.91*
Median	*24*	*38*	*39*	*47*	*34*	*36.5*	*38*	*32*	*37.5*	*38*	*14.5*	*9*	*37.5*
Skewness	*0.46*	*0.25*	*0.14*	*−0.02*	*−0.02*	*0.52*	*0.29*	*−0.28*	*−0.44*	*0.04*	*0.40*	*0.30*	*0.39*
Kurtosis	*−0.15*	*−0.37*	*−0.86*	*−0.11*	*−0.13*	*−0.87*	*−0.28*	*−0.59*	*−0.98*	*−0.43*	*−0.70*	*−0.63*	*0.02*
Geom. mean	*24.78*	*38.40*	*39.00*	*46.74*	*32.50*	*36.78*	*38.32*	*30.89*	*36.76*	*37.25*	*15.09*	*8.16*	*34.95*
Lead													
N	*70*	*139*	*12*	*18*	*191*	*18*	*29*	*34*	*19*	*38*	*11*	*60*	*20*
Min	*11*	*9*	*20*	*14*	*9*	*10*	*8*	*9*	*13*	*7*	*15*	*5*	*6*
Max	*31*	*27*	*23*	*24*	*28*	*30*	*27*	*32*	*25*	*20*	*18*	*23*	*24*
Sum	*1451*	*2352*	*258*	*334*	*3296*	*374*	*499*	*624*	*379*	*509*	*183*	*742*	*327*
Mean	*20.73*	*16.92*	*21.50*	*18.56*	*17.26*	*20.78*	*17.21*	*18.35*	*19.95*	*13.39*	*16.64*	*12.37*	*16.35*
Std. error	*0.60*	*0.34*	*0.26*	*0.62*	*0.31*	*1.30*	*0.85*	*0.95*	*0.81*	*0.51*	*0.24*	*0.51*	*0.99*
Variance	*25.13*	*16.39*	*0.82*	*6.97*	*18.52*	*30.65*	*20.88*	*30.48*	*12.39*	*9.98*	*0.65*	*15.86*	*19.71*
Stand. dev	*5.01*	*4.05*	*0.90*	*2.64*	*4.30*	*5.54*	*4.57*	*5.52*	*3.52*	*3.16*	*0.81*	*3.98*	*4.44*
Median	*21*	*17*	*22*	*19*	*17*	*19*	*17*	*17.5*	*19*	*13*	*17*	*12*	*16*
Skewness	*−0.31*	*0.15*	*−0.34*	*0.06*	*0.55*	*0.22*	*0.46*	*0.66*	*−0.04*	*0.21*	*−0.40*	*0.45*	*−0.35*
Kurtosis	*−0.67*	*−0.69*	*−1.04*	*−0.84*	*−0.43*	*−0.87*	*−0.22*	*−0.26*	*−1.11*	*−0.52*	*−0.62*	*0.11*	*−0.31*
Geom. mean	*20.06*	*16.43*	*21.48*	*18.38*	*16.74*	*20.06*	*16.62*	*17.59*	*19.64*	*13.02*	*16.62*	*11.72*	*15.66*

positive correlation between trace metal concentration and the proportion of fine-grained material in alluvial sediment (Förstner and Wittmann, 1979; Förstner, 1982; Rubio et al., 2000; Dypvik and Harris, 2001; Singh and Rajamani, 2001; Whitmore et al., 2004; Wyżga and Ciszewski, 2010). This trend is due to textural modifications that occur while fluvial sediment undergoes hydraulic selection and sorting with increasing distance from the channel.

In the study area, natural metal contents are clearly affected by grain size variations, and several observed compositional changes can be related to changes from low-energy to high-energy depositional

environments. For example, clay delta plain deposits (GFU A4 in Fig. 3, left) display systematically higher Cr contents than silt–sand distributary channel–levee facies associations (B4 and B6). The latter, in turn, are enriched in metals compared to the sandier delta front sediments (GFU C2). The same holds for sediment supplied by non-ophiolitic sources. Metal concentrations are highest in the finest-grained fraction (GFU A2 in Fig. 3, left), whereas beach sands fed by Apenninic rivers exhibit comparatively lower Cr values (GFU C1).

The influence of grain size on metal distribution is even more obvious for those metals that are not much sensitive to changes in parent-rock composition, such as Zn (Fig. 3, right) and Cu (Fig. 4). Unlike for Cr, almost all samples in the Zn/V diagram plot along a single, well defined regression line, irrespective of the ophiolitic versus non-ophiolitic source-rock contribution (Fig. 3, right). If grouped according to the dominant sedimentary process, with no distinction between fluvial and deltaic deposits, overbank fines (GFUs A2–A4), channel-related sands and silts (B1–B6) and nearshore sands (C1–C2) plot into distinct fields of the Zn/V diagram, with poor overlap. This distribution highlights the influence of selective transport on metal distribution.

5.3. Degree of soil weathering

Owing to much reduced time of subaerial exposure, the degree of soil weathering of post-Roman age (<2 ky BP) alluvial, deltaic and coastal deposits is generally low (Arenosols of WRB IUSS Working Group, 2006) or moderate (Cambisols, Calcisols and Vertisols of WRB IUSS Working Group, 2006). An exception are pre-Holocene soil units (GFU A1), cropping out at the basin margin (Fig. 2), which were exposed from their time of formation for a period of several tens of thousands of years. The longer time of subaerial exposure, which implies higher degree of weathering, is reflected by a diagnostic pedological (argillic horizon) and geochemical signature, including characteristic losses of Zn and Cu with respect to the younger, and less weathered soils (Fig. 3, right and Fig. 4). This is due to a reduction in mineral diversity through progressive dissolution of unstable mineral species. Conversely, Cr is slightly enriched in residual mineral phases (see A1 in Fig. 4).

6. Mapping the natural background content

The pedogeochemical map of the Emilia-Romagna plain (Fig. 5) depicts the subsoil (90–140 cm) natural spatial distribution of five potentially toxic metals (Cr, Ni, Zn, Cu and Pb) in soils for agricultural use. In these maps, the GFUs were grouped into four classes of metal concentration, centred on the threshold limit values (x) for each metal (red lines in Fig. 4). The lower two classes in each map are separated by a metal content equal to x/2, while the upper two classes are separated by a metal content equal to 3/2x. Darker shades on map denote natural concentrations exceeding the Italian threshold values, whereas lighter shades indicate natural metal contents below these limits (Fig. 5). The 95th percentile metal concentration for the 90–140 cm population of each GFU (see Fig. 4) represents an upper threshold value to that specific geological/pedological domain, and was selected as default natural background value (Ander et al., 2013).

Source-rock composition appears to be the primary control on the natural spatial distribution of Cr and Ni within the soils of the Emilia-Romagna plain (Fig. 5). In particular, the highest Cr and Ni concentrations are recorded in sediment supplied by erosion of Alpine and Apenninic ultramafic complexes (compare with Fig. 1). Cr- and Ni-rich areas include the Po River, the abandoned Po Delta lobe and several river systems from the western (Emilia) Apennines (between Trebbia and Taro rivers in Fig. 1).

It is remarkable that in all areas supplied by ophiolite-rich sources, natural Cr and Ni concentrations lie by a good margin above the threshold values (150 mg/kg for Cr, 120 mg/kg for Ni — see Fig. 4). Where the ophiolitic detritus makes up a substantial part of sediment composition, such as in the case of GFU B5, Cr concentrations can even be up to 4–5 times higher than those limits (maximum value: 646 mg/kg; median value: 345 mg/kg in Table 2), whereas Ni concentrations can be three times higher (maximum value: 387 mg/kg; median value: 207 mg/kg in Table 2). According to the Italian regulations, this part of the Po Plain is regarded as a polluted area. By contrast, Cr and Ni contents well below the maximum permissible concentrations are recorded where the drainage basins are ophiolite-free (e.g., Romagna Apennines).

Within each distinct provenance domain, Cr (and Ni) distribution is markedly size dependent (Figs. 3, 4 and 5). In particular, sediment

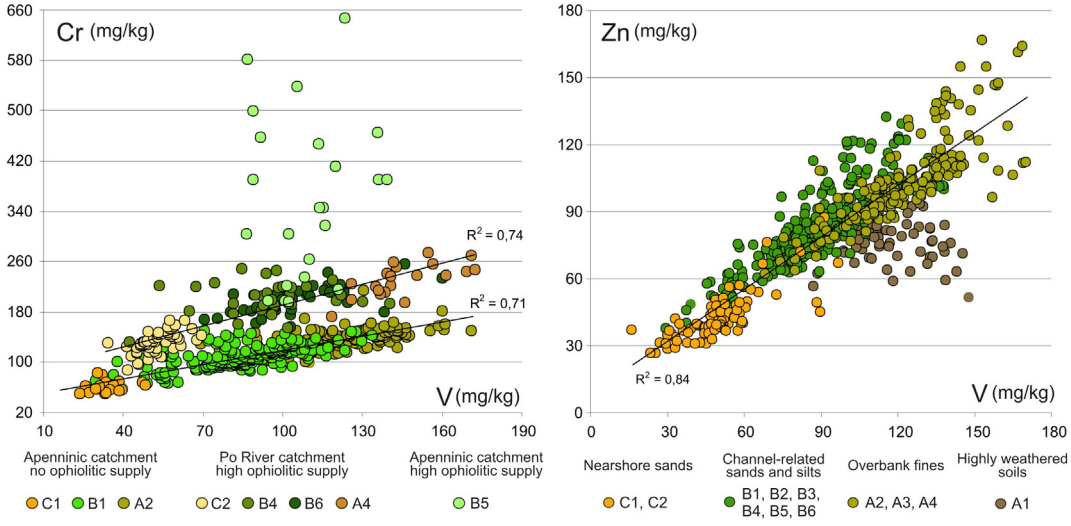

Fig. 3. Left: Scatterplots of V versus Cr from 526 samples at 90–140 cm depth, showing natural metal concentrations as a function of sediment provenance and grain size. Samples from non-ophiolitic sources (lower regression line) exhibit systematically lower Cr contents than samples from highly-ophiolitic catchments (upper regression line + GFU B5). Natural Cr contents generally increase with increasing clay proportion, along both regression lines (C1 to A2 and C2 to A4). Right: Positive covariance of V/Zn based upon 668 samples at 90–140 cm depth. As for Cr, higher Zn values are invariably recorded in finer-grained (floodplain and swamp) deposits (GFUs A2–A4) relative to their coarser-grained counterparts (channel-related and beach facies – GFUs B1–B6 and UGFs C1–C2). Also note Zn depletion as a function of increasing degree of soil weathering (GFU A1 = pre-Holocene deposits). For GFU codes and description, see Table 1.

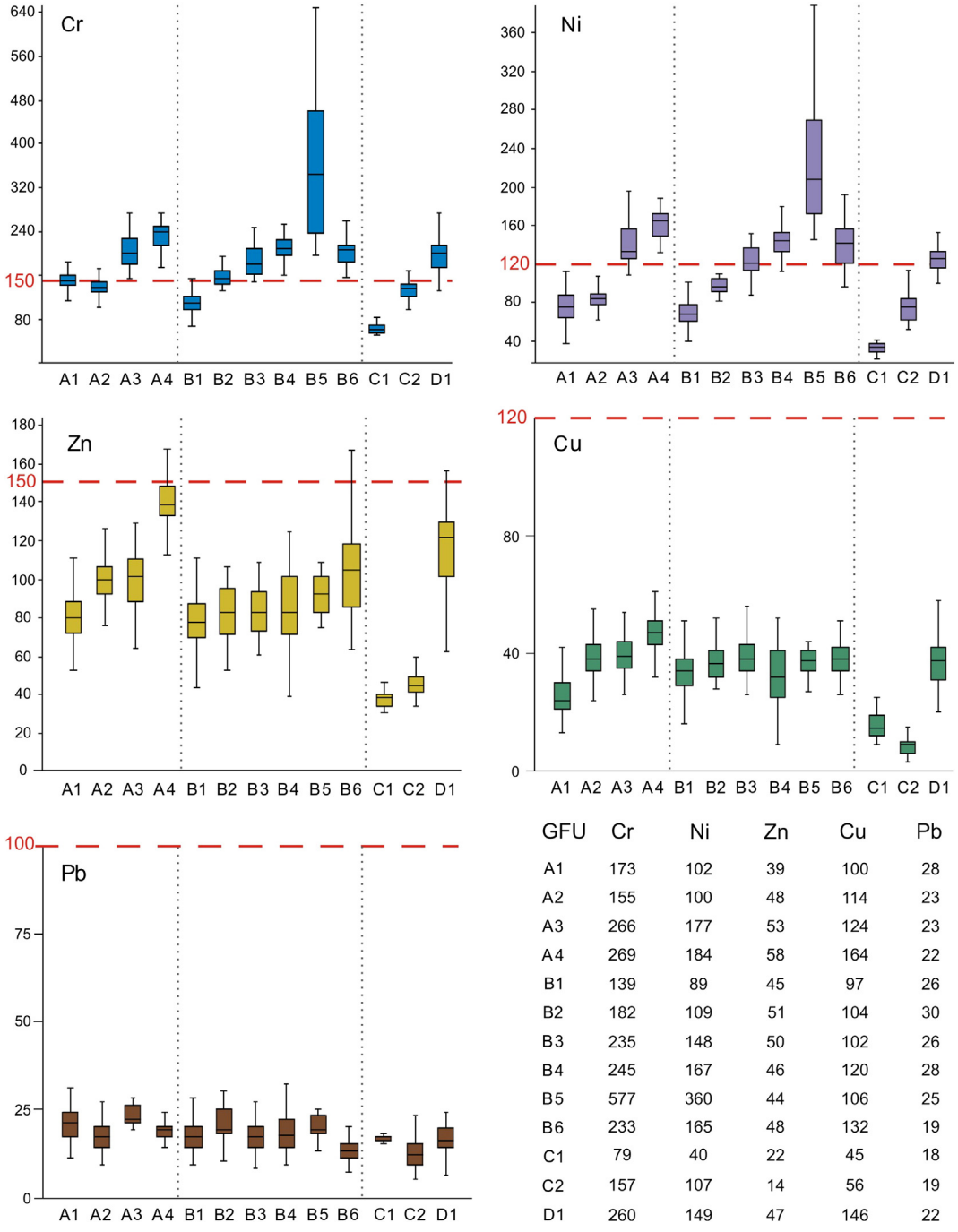

GFU	Cr	Ni	Zn	Cu	Pb
A1	173	102	39	100	28
A2	155	100	48	114	23
A3	266	177	53	124	23
A4	269	184	58	164	22
B1	139	89	45	97	26
B2	182	109	51	104	30
B3	235	148	50	102	26
B4	245	167	46	120	28
B5	577	360	44	106	25
B6	233	165	48	132	19
C1	79	40	22	45	18
C2	157	107	14	56	19
D1	260	149	47	146	22

Fig. 4. Box-and-whiskers plots, showing natural metal distribution (Cr, Ni, Zn, Cu and Pb) in the 13 genetic and functional soil units (for GFU description, see Table 1). The red dashed lines indicate the threshold values for uncontaminated lands, according to the Italian regulations. The lower boundary of each box is the 25th percentile, the upper boundary is the 75th percentile, the bold line within the box corresponds to the median, the "whiskers" define the minimum and maximum values. Numbers in the lower right corner correspond to 95th percentile metal concentrations (mg/kg), calculated for each GFU following statistical analysis. These numbers, which represent upper threshold metal values for each GFU, were used for building the pedogeochemical maps of Fig. 5. (For interpretation of the references to color in this figure legend, the reader is referred to the web version of this article.)

undergoes hydraulic selection and sorting during transport, and significant changes in metal concentrations are observed as a function of the different sedimentary facies. Metals supplied to the alluvial and coastal plain are generally concentrated in the finest sediment fraction (floodplain, bay and swamp clays and silts), whereas near-channel (crevasse and overbank) deposits exhibit invariably lower metal contents. Beach-ridge sands display the lowest metal concentrations (compare Fig. 5 with Fig. 2).

Metals other than Cr and Ni behave differently. In these instances, spatial metal distribution does not reflect major differences in sediment provenance, but is instead primarily a function of grain size variability and/or degree of soil weathering. In particular, Zn is notably enriched within the fine-grained (floodplain, interdistributary) GFUs (A2, A3, and especially A4 in Fig. 4), whereas it exhibits comparatively lower values within the coarser, channel-related facies (GFUs "B"). Distributary channel (i.e., deltaic) samples (GFU B6) exhibit relatively higher Zn concentrations than their proximal fluvial-channel counterpart (GFU B4). The lowest Zn values are recorded within coarse-grained littoral sands (GFUs "C").

As for Cr, Ni and Zn, Cu is strongly depleted within coastal sandy soils (GFUs "C" in Fig. 4), but also reveals deficiency in highly altered soils (GFU A1), in response to leaching processes. Finally, the spatial

distribution of Pb appears rather homogeneous across the study area (Fig. 4) and possible changes as a function of grain size are below the instrument resolution. Both Cu and Pb contents are invariably well below the threshold values (Fig. 5).

Through geochemical fingerprinting of distinct sedimentary and soil units (Fig. 4) and the construction of a new type of (soil- and geologically-oriented) geochemical map (Fig. 5), we document that reliable prediction of superficial natural metal distribution is possible (also see Spadoni et al., 2007). The pedogeochemical map of the Emilia-Romagna plain uses a combination of geological and pedological concepts to define separate natural metal concentrations representative of each soil unit (= GFU), instead of a unique, pre-determined threshold value. A key difference with the geochemical maps built on geostatistical interpolation methods alone relies on the delineation of boundaries between concentration classes: in our map, these boundaries largely coincide with observed (soil/geological unit), rather than inferred map boundaries (compare Fig. 5 with Fig. 2). Sharp concentration changes are systematically observed across the major geological and soil boundaries, but a high degree of spatial continuity and consistency is expected within those boundaries (Cohen et al., 2012). The pedogeochemical map can thus be used as a powerful tool to estimate geochemical patterns where analytical data are missing.

7. Natural metal background and anthropogenic pollution

The pollution status of a soil can efficiently be evaluated through comparison between topsoil metal concentrations and natural background values, i.e., current and pre-industrial concentrations, respectively. To this purpose, the most commonly calculated parameter is the Index of geoaccumulation, Igeo (Müller, 1979; Förstner and Müller, 1981), defined as

$$\mathrm{Igeo} = \log_2 \mathrm{Cn}/(1.5 * \mathrm{Bn})$$

where Cn is the measured metal content and Bn is the mean concentration of the Earth's crust. On the basis of distinct Igeo values, the pollution status of a soil can be differentiated into seven classes (Förstner and Müller, 1981; Rubio et al., 2000; Banat et al., 2005; Sainz and Ruiz,

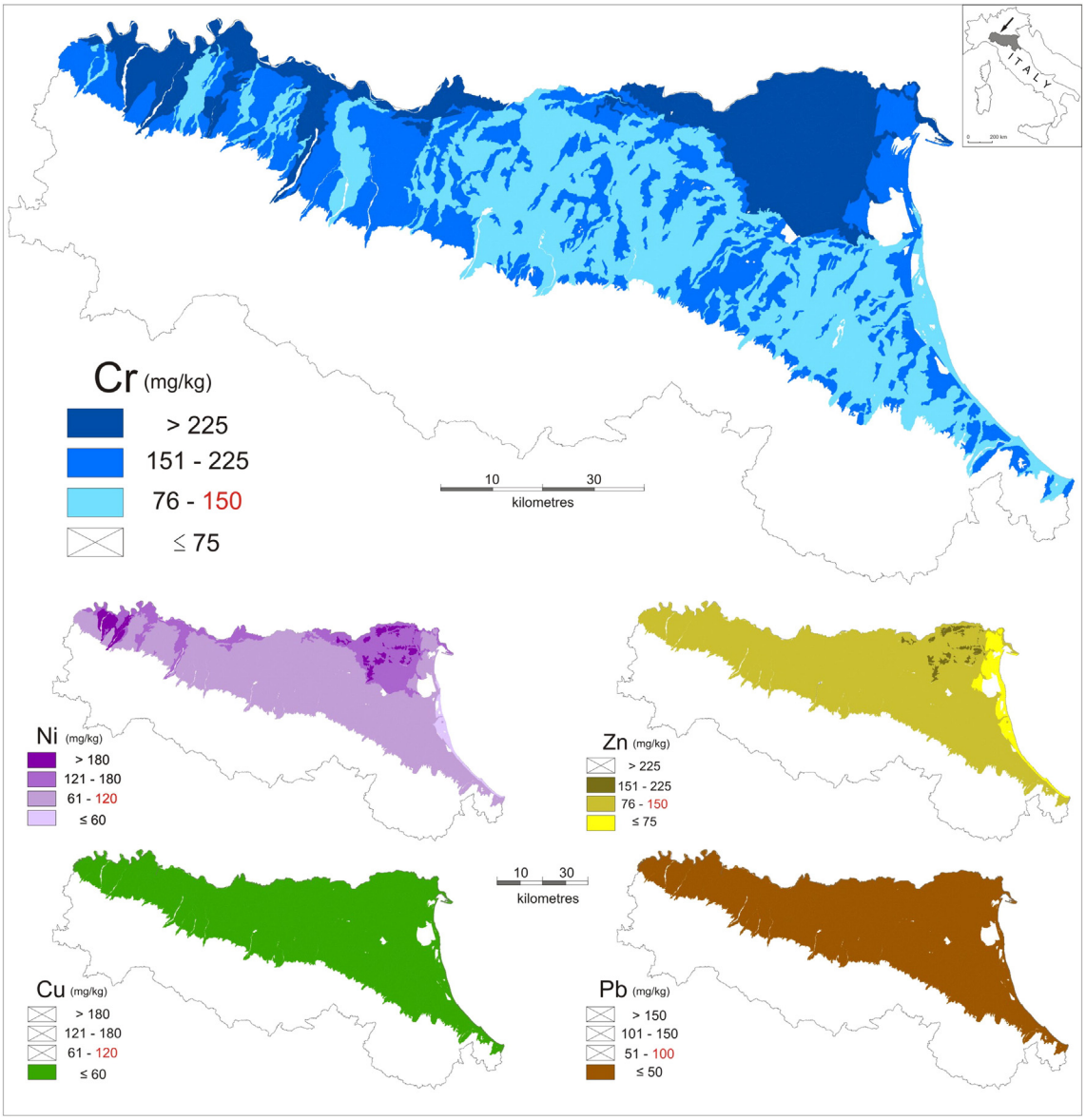

Fig. 5. Pedogeochemical maps of Cr, Ni, Zn, Cu and Pb, depicting natural metal concentrations in the Emilia-Romagna plain (the 95th percentile values of Fig. 4 are selected as default natural background concentrations). The red numbers define the Italian threshold values. Boundaries on map coincide with physical (soil/geological unit) boundaries (compare with Fig. 2). The geographical boundary is the Emilia-Romagna region border. (For interpretation of the references to color in this figure legend, the reader is referred to the web version of this article.)

2006), from unpolluted (≤0) to extremely polluted (>5). In this study, we used the metal concentrations in topsoil samples (at 20–30 cm depth) as Cn, while the natural background value of the same metal at 90–140 cm depth was taken as Bn.

As clearly documented by the invariably negative I_{geo} values recorded throughout the southern Po Plain (green dots in Fig. 6A), despite very high local concentrations, commonly exceeding the threshold limit values for contaminated lands, we did not observe any remarkable enrichment in Cr (or Ni) within topsoil samples. Such negative I_{geo} values lead us to conclude that the study area is not polluted for any of these metals. An opposite behavior is shown by Cu (Fig. 6B). For this metal, despite generally low concentrations a moderate, but diffuse contamination across a significant part of the southern Po Plain is suggested by higher I_{geo} values, commonly in the range of 0–2 (Fig. 6B).

The maps of the geochemical anomalies shown in Fig. 6 are dot density maps, built on point information obtained from individual study sites. For this reason, they cannot be extrapolated outside such small areas. In order to detect precisely the sources of anthropogenic contamination specific, local studies should be undertaken. However, these maps provide an overview of the pollution state of soils.

For Cr and Ni, >98% of the samples in the study area exhibit no pollution (Fig. 7), and it is apparent from field data that the remaining 2% is naturally enriched due to vertical (textural or provenance) change from topsoil to subsoil samples (see Grygar et al., 2013). Nor the studied soils display important contamination for Zn (93% neutral values of Igeo). Pb and Cu offer, instead, a different picture: unpolluted soils decrease to 72% for Pb, and to less than 60% for Cu (Fig. 7). It is conceivable that contributors to this superficial enrichment in Cu are pesticides for vineyards and vast quantities of pig slurries.

In general terms, as shown from different regions (Steinnes, 2001), this study demonstrates that high Cr and Ni concentrations in the topsoils of the Emilia-Romagna plain do not necessarily imply anthropogenic influence. Conversely, even where the measured topsoil metal concentrations are well below the threshold limit values, such as in the case of Cu, many areas are impacted and show a state of diffuse contamination.

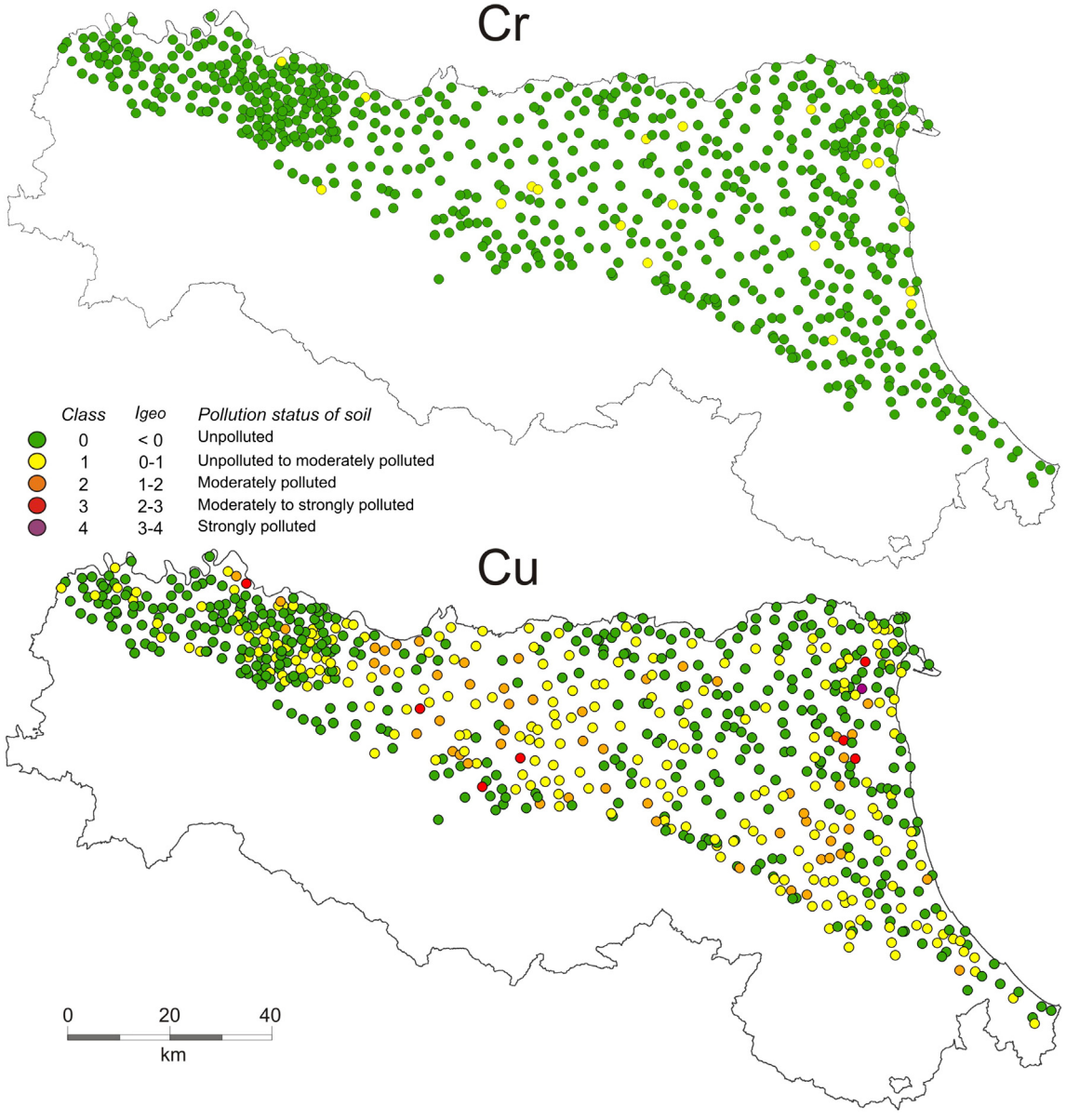

Fig. 6. Geochemical anomalies of Cr (A) and Cu (B) in the Emilia-Romagna plain. Igeo classes after Müller (1979). The geographical boundary is the Emilia-Romagna border.

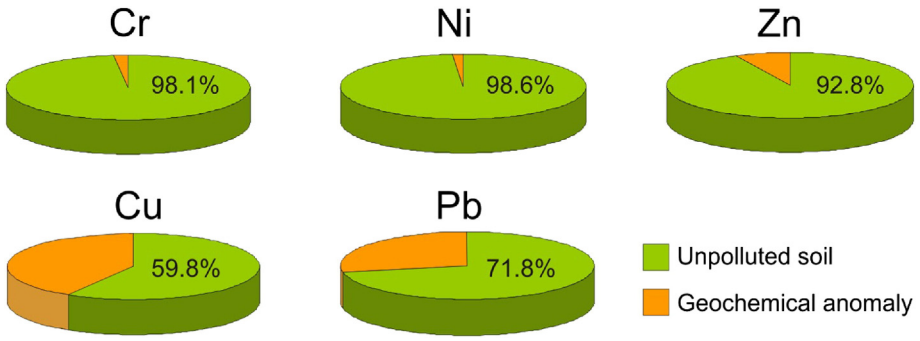

Fig. 7. Percentage distribution of unpolluted soils and geochemical anomalies, as revealed by the Geoaccumulation Index calculated from 707 sampling sites.

8. Conclusions

The pedogeochemical map of the Emilia-Romagna plain represents the first step toward a new type of geochemical map that can be used pragmatically by the regulatory bodies to deal with environmental protection issues.

Sedimentological, pedological and geochemical analyses of 1414 soil samples enable precise identification of the natural contents of selected potentially harmful heavy metals (Cr, Ni, Cu, Zn, Pb) as a function of sediment provenance, soil texture and degree of soil weathering. Thirteen Genetic and functional soil units (GFUs), each bearing a distinctive connotation in terms of soil profile, weathering, grain size and sediment source, were defined on map and used as reference units for geochemical characterization. Accurate facies analysis allowed precise attribution of each GFU to specific depositional processes and sub-environments. Statistical analysis was performed through cluster analysis, frequency histograms, cumulative frequency curves, and box-and-whiskers plots. The Kolmogorov–Smirnov test was used to determine the type of data distribution. For dataset that did not follow a normal distribution, Box–Cox transformations were used.

Source-rock composition proves to be the primary control on the natural spatial distribution of Cr and Ni: sediment deriving from erosion of Alpine and Apenninic ultramafic complexes invariably contains high concentrations of these environmentally important trace elements. In contrast, significantly lower Cr and Ni contents are recorded where the drainage basins are ophiolite-free (e.g., Romagna Apennines). The spatial distribution of other potentially toxic metals in the Emilia-Romagna plain does not reflect major differences in sediment provenance, but is instead primarily a function of changes in grain size and degree of soil weathering. In particular, Zn and Cu are notably enriched within fine-grained fluvial and deltaic deposits, whereas they exhibit generally lower values within their coarse-grained (fluvial- and distributary channel) counterparts, and display the lowest values within coarse sandy littoral sands. Concentrations of Cu and Zn also show deficiencies in highly altered soils, in response to leaching processes. The spatial distribution of Pb is rather homogeneous across the study area.

A realistic view of the pollution status of soils was obtained by matching the pedogeochemical contents estimated from subsoil samples against the metal contents recorded in the corresponding topsoil samples. Cr and Ni concentrations above the threshold values designated for contaminated areas mostly reflect catchment geology, and are not the product of anthropogenic pollution. In contrast, diffuse (albeit moderate) topsoil contamination was demonstrated for Cu, even though measured metal concentrations lie below the admissible levels. The inadequacy of regulations based on pre-determined threshold values is thus documented.

In this paper, we show that natural metal concentrations in alluvial and coastal plain deposits are narrowly related to soil properties and that, for this reason, integrated sedimentological and soil studies constitute a priority for geochemical mapping. Delineating a geochemical signature for specific soil typological units and sedimentary facies is imperative to obtain realistic information about the natural distribution of potentially toxic metals. An appropriate sampling strategy, including detailed soil characterization is recommended to adequately represent the remarkable variability in terms of source-rock composition, grain size and degree of soil weathering. Soil-oriented geochemical maps represent an efficient alternative approach to conventional geochemical mapping based upon geostatistical methods alone. Specifically, through the geochemical characterization of genetic-functional soil units, the pedogeochemical map of the Emilia-Romagna plain constitutes a powerful tool to assess the anthropogenic impact on soils, which can be of use for legislative purposes and planning strategies for environmental protection.

Acknowledgments

This project was financially supported by the Geological, Seismic and Soil Survey of Regione Emilia-Romagna (grant numbers: 2372/2008, 2205/2009, 16142/2012, and 16270/2013) (thanks to Raffaele Pignone). We are deeply indebted to four anonymous reviewers for their insightful suggestions which greatly improved our paper.

References

Albanese S, De Vivo B, Lima A, Cicchella D. Geochemical background and baseline values of toxic elements in stream sediments of Campania region (Italy). J Geochem Explor 2007;93:21–34.

Amorosi A. Chromium and nickel as indicators of source-to-sink sediment transfer in a Holocene alluvial and coastal system (Po Plain, Italy). Sediment Geol 2012;280:260–9.

Amorosi A, Sammartino I. Influence of sediment provenance on background values of potentially toxic metals from near-surface sediments of Po coastal plain (Italy). Int J Earth Sci 2007;96:389–96.

Amorosi A, Sammartino I. Assessing natural contents of hazardous metals by different analytical methods and its impact on environmental legislative measures. Int J Environ Pollut 2011;46:164–77.

Amorosi A, Centineo MC, Dinelli E, Lucchini F, Tateo F. Geochemical and mineralogical variations as indicators of provenance changes in Late Quaternary deposits of SE Po Plain. Sediment Geol 2002;151:273–92.

Amorosi A, Colalongo ML, Dinelli E, Lucchini F, Vaiani SC. Cyclic variations in sediment provenance from late Pleistocene deposits of the eastern Po Plain, Italy. In: Arribas J, Critelli S, Johnsson MJ, editors. Sedimentary Provenance and Petrogenesis: Perspectives from Petrography and Geochemistry, 420. Geological Society of America; 2007. p. 13–24. [Special Paper].

Amorosi A, Dinelli E, Rossi V, Vaiani SC, Sacchetto M. Late Quaternary palaeoenvironmental evolution of the Adriatic coastal plain and the onset of Po River Delta. Palaeogeogr Palaeoclimatol 2008;268:80–90.

Amorosi A, Bruno L, Rossi V, Severi P, Hajdas I. Paleosol architecture of a late Quaternary basin–margin sequence and its implications for high-resolution, non-marine sequence stratigraphy. Global Planet Change 2014;112:12–25.

Ander EL, Johnson CC, Cave MR, Palumbo-Roe B, Nathanail CP, Lark RM. Methodology for the determination of normal background concentrations of contaminants in English soil. Sci Total Environ 2013;454–455:604–18.

APAT. Protocollo operativo per la determinazione dei valori di fondo di metalli/metalloidi nei suoli e dei siti d'interesse nazionale. Roma: Agenzia per la Protezione dell'Ambiente e per i Servizi Tecnici; 2006.

ARPAV. Metalli e metalloidi nei suoli del Veneto – Determinazione dei valori di fondo. Dipartimento Provinciale di Treviso - Servizio Suoli, Regione Veneto; 2011.

Banat KM, Howari FM, Al-Hamad AA. Heavy metals in urban soils of central Jordan: should we worry about their environmental risks? Environ Res 2005;97:258–73.
Bianchini G, Laviano R, Lovo S, Vaccaro C. Chemical mineralogical characterisation of clay sediments around Ferrara (Italy): a tool for environmental analysis. Appl Clay Sci 2002;21:165–76.
Bianchini G, Di Giuseppe D, Natali C, Beccaluva L. Ophiolite inheritance in the Po Plain sediments: insights on heavy metals distribution and risk assessment. Ofioliti 2013; 38:1–14.
Bianchini G, Cremonini S, Di Giuseppe D, Vianello G, Vittori Antisari L. Multiproxy investigation of a Holocene sedimentary sequence near Ferrara (Italy): clues on the physiographic evolution of the eastern Padanian Plain. J Soils Sediment 2014;14: 230–42.
Blaser P, Zimmermann S, Luster J, Shotyk W. Critical examination of trace element enrichments and depletions in soils: As, Cr, Cu, Ni, Pb and Zn in Swiss forest soils. Sci Total Environ 2000;249:257–80.
Bondesan M, Favero V, Viñals MJ. New evidence on the evolution of the Po-delta coastal plain during the Holocene. Quatern Int 1995;29–30:105–10.
Cheng Q. Mapping singularities with stream sediment geochemical data for prediction of undiscovered mineral deposits in Gejiu, Yunnan Province, China. Ore Geol Rev 2007; 32:314–24.
Cicchella D, De Vivo B, Lima A. Background and baseline concentration values of elements harmful to human health in the volcanic soils of the metropolitan provincial area of Napoli (Italy). Geochem Explor Environ Anal 2005;5:29–40.
Cohen DR, Rutherford NF, Morisseau E, Zissimos AM. Geochemical patterns in the soils of Cyprus. Sci Total Environ 2012;420:250–62.
Correggiari A, Cattaneo A, Trincardi F. Depositional patterns in the Holocene Po Delta system. In: Bhattacharya JP, Giosan L, editors. River Deltas: Concepts, Models and Examples, 83. Society of Economic Paleontologists and Mineralogists; 2005. p. 365–92. [Special Publication].
Covelli S, Fontolan G. Application of a normalization procedure in determining regional geochemical baselines, Gulf of Trieste, Italy. Environ Geol 1997;30:34–45.
Curzi PV, Dinelli E, Ricci Lucchi M, Vaiani SC. Palaeoenvironmental control on sediment composition and provenance in the late Quaternary deltaic successions: a case study from the Po delta area (Northern Italy). Geol J 2006;41:591–612.
Darnley AG. A global geochemical reference network: the foundation for geochemical baselines. J Geochem Explor 1997;60:1–5.
Daskalakis KD, O'Connor TP. Normalization and elemental sediment contamination in the coastal United States. Environ Sci Technol 1995;29:470–7.
Dinelli E, Tateo F, Summa V. Geochemical and mineralogical proxies for grain size in mudstones and siltstones from the Pleistocene and Holocene of the Po River alluvial plain, Italy. In: Arribas J, Critelli S, Johnsson MJ, editors. Sedimentary Provenance and Petrogenesis: Perspectives from Petrography and Geochemistry, 420. Geological Society of America; 2007. p. 25–36. [Special Paper].
Dypvik H, Harris NB. Geochemical facies analysis of fine-grained siliciclastics using Th/U, Zr/Rb and (Zr + Rb)/Sr ratios. Chem Geol 2001;181:131–46.
Förstner U. Accumulative phases for heavy metals in limnic sediments. Hydrobiologia 1982;91:269–84.
Förstner U, Müller G. Concentrations of heavy metals and polyciclic aromatic hydrocarbons in river sediments: geochemical background, man's influence and environmental impact. GeoJournal 1981;5:417–32.
Förstner U, Wittmann GTW. Metal Pollution in the Aquatic Environment. New York: Springer-Verlag; 1979.
Franzini M, Leoni L, Saitta M. A simple method to evaluate the matrix effects in X-ray fluorescence analysis. X-Ray Spectrom 1972;1:150–4.
Garcia D, Ravenne C, Maréchal B, Moutte J. Geochemical variability induced by entrainment sorting: quantified signals for provenance analysis. Sediment Geol 2004;171: 113–28.
Garzanti E, Andò S, Vezzoli G. Grain-size dependence of sediment composition and environmental bias in provenance studies. Earth Planet Sci Lett 2009;277:422–32.
Govindarajiu K. Compilation of working values and sample description for 272 geostandards. Geostand Newslett 1989;13:1–114.
Grygar TM, Nováková T, Bábek O, Elznicová J, Vadinová N. Robust assessment of moderate heavy metal contamination levels in floodplain sediments: a case study on the Jizera River, Czech Republic. Sci Total Environ 2013;452–453:233–45.
Gunderson KL, Pazzaglia FJ, Picotti V, Anastasio DA, Kodama KP, Rittenour T, et al. Unraveling tectonic and climatic controls on synorogenic growth strata (Northern Apennines, Italy). Geol Soc Am Bull 2014;126:532–52.
Hiscott RN. Ophiolitic source rocks for Taconic-age flysch: trace-element evidence. Geol Soc Am Bull 1984;95:1261–7.
Huisman DJ, Vermeulen FJH, Baker J, Veldkamp A, Kroonenberg SB, Klaver GTh. A geological interpretation of heavy metal concentrations in soils and sediments in the southern Netherlands. J Geochem Explor 1997;59:163–74.
ISO 19258. Soil Quality — Guidance on the Determination of Background Values; 2005.
Leoni L, Menichini M, Saitta M. Determination of S, Cl and F in silicate rocks by X-ray fluorescence analysis. X-Ray Spectrom 1982;11:156–8.
Lepeltier C. A simplified statistical treatment of geochemical data by graphical representation. Econ Geol 1969;64:538–50.
Liaghati T, Preda M, Cox M. Heavy metal distribution and controlling factors within coastal plain sediments, Bells Creek catchment, southeast Queensland, Australia. Environ Int 2003;29:935–48.
Loring DH. Normalization of heavy-metal data from estuarine and coastal sediments. ICES J Mar Sci 1991;48:101–15.
Marchesini L, Amorosi A, Cibin U, Zuffa GG, Spadafora E, Preti D. Sand composition and sedimentary evolution of a Late Quaternary depositional sequence, northwestern Adriatic Coast, Italy. J Sediment Res 2000;70:829–38.
Menon MG, Gibbs RJ, Phillips A. Accumulation of muds and metals in the Hudson River Estuary turbidity maximum. Environ Geol 1998;34:214–22.
Micó C, Recatalá L, Sánchez J. Statistical approaches to establish background values of potentially toxic elements. In: Dominguez JB, editor. Soil Contamination Research Trends. Hauppauge, New York: Nova Science Publishers, Inc; 2008. p. 217–34.
Morton AC, Hallsworth CR. Processes controlling the composition of detrital heavy mineral assemblages in sandstones. Sediment Geol 1999;124:3–29.
Müller G. Schwermetalle in den Sedimenten des Rheins-Veränderungen seit 1971. Umscham 1979;79:778–83.
Ori GG. Continental depositional systems of the Quaternary of the Po plain (northern Italy). Sediment Geol 1993;83:1–14.
Picotti V, Pazzaglia FJ. A new active tectonic model for the construction of the Northern Apennines mountain front near Bologna (Italy). J Geophys Res 2008;113:B08412. http://dx.doi.org/10.1029/2007JB005307.
Pini GA. Tectonosomes and olistostromes in the Argille Scagliose of the northern Apennines, Italy. Geol Soc Am Spec Pap 1999;335. [Boulder, Colorado].
Plant JA, Klaver G, Locutura J, Salminen R, Vrana K, Fordyce FM. The Forum of European Geological Surveys Geochemistry Task Group inventory 1994–1996. J Geochem Explor 1997;59:123–46.
Ratcliffe KT, Morton AC, Ritcey DH, Evenchick CA. Whole-rock geochemistry and heavy mineral analysis as petroleum exploration tools in the Bowser and Sustut basins, British Columbia, Canada. B Can Petrol Geol 2007;55:320–36.
Regione Emilia-Romagna. Carta dei Suoli della Pianura emiliano-romagnola in scala 1:50. 000. Guermandi M, Tarocco P, editors. Geological, Seismic and Soil Survey, Regione Emilia-Romagna, Bologna; 2010.
Regione Emilia-Romagna. Carta geologica di pianura dell'Emilia-Romagna alla scala 1: 250.000. Preti D, editor. Geological Survey of Regione Emilia-Romagna, Bologna; 1999.
Regione Emilia-Romagna. The Pedogeochemical Map of the Emilia-Romagna plain (1:250,000 scale). Amorosi A, Guermandi M, Marchi N, Sammartino I, editors. Geological, Seismic and Soil Survey, Regione Emilia-Romagna, Bologna; 2012. (http://ambiente.regione.emilia-romagna.it/geologia-en/temi/heavy-metals-in-soil)
Reimann C, Filzmoser P. Normal and lognormal data distribution in geochemistry: death of a myth. Consequences for the statistical treatment of geochemical and environmental data. Environ Geol 2000;39:1001–14.
Reimann C, Garrett RG. Geochemical background — concept and reality. Sci Total Environ 2005;350:12–27.
Reimann C, Filzmoser P, Garrett RG. Factor analysis applied to regional geochemical data: problems and possibilities. Appl Geochem 2002;17:185–206.
Ricci Lucchi F. Oligocene to Recent foreland basins of northern Apennines. In: Ph Allen, Homewood P, editors. Foreland Basins, 8. International Association of Sedimentologists; 1986. p. 105–39. [Special Publication].
Rose AW, Hawkes HE, Webb JS. Geochemistry in Mineral Exploration. 2nd ed. New York: Academic Press; 1979.
Rubio B, Nombela MA, Vilas F. Geochemistry of major and trace elements in geochemistry of de Ria de Vigo (NW Spain): an assessment of metal pollution. Mar Pollut Bull 2000; 40:968–80.
Sainz A, Ruiz F. Influence of the very polluted inputs of the Tinto–Odiel system on the adjacent littoral sediments of southwestern Spain: a statistical approach. Chemosphere 2006;62:1612–22.
Salminen R, Tarvainen T. The problem of defining geochemical baselines. A case study of selected elements and geological materials in Finland. J Geochem Explor 1997;60:91–8.
Singh P, Rajamani V. Geochemistry of the floodplain sediments of the Kaveri river, southern India. J Sediment Res 2001;71:50–60.
Spadoni M, Voltaggio M, Carcea M, Coni E, Raggi A, Cubadda F. Bioaccessible selenium in Italian agricultural soils: comparison of the biogeochemical approach with a regression model based on geochemical and pedoclimatic variables. Sci Total Environ 2007;376:160–77.
Steinnes E. Metal contamination of the natural environment in Norway from long range atmospheric transport. Water Air Soil Pollut 2001;1:449–60.
Sterckemann T, Gomez A, Ciesielski H. Soil and waste analysis for environmental risk assessment in France. Sci Total Environ 1996;178:63–9.
Tarvainen T, Kallio E. Baselines of certain bioavailable and total heavy metal concentrations in Finland. Appl Geochem 2002;17:975–80.
Tarvainen T, Jarva J, Kahelin H. Geochemical baselines in relation to analytical methods in the Itä-Uusimaa and Pirkanmaa regions, Finland. Geochem Explor Environ Anal 2009;9:81–92.
Veggiani A. Le variazioni idrografiche del basso corso del fiume Po negli ultimi 3000 anni. Padusa 1974;1–2:39–60.
Whitmore GP, Crook KAW, Johnson DP. Grain size control of mineralogy and geochemistry in modern river sediment, New Guinea collision, Papua New Guinea. Sediment Geol 2004;171:129–57.
WRB IUSS Working Group. World reference base for soil resources; 2006 [World Soil Resources Reports 103, FAO, Rome; 2006].
Wyżga B, Ciszewski D. Hydraulic controls on the entrapment of heavy metal-polluted sediments on a floodplain of variable width, the upper Vistula River, southern Poland. Geomorphology 2010;117:272–86.